

# Raman spectroscopy of InN films grown on Si

F. Agulló-Rueda\*

*Instituto de Ciencia de Materiales de Madrid (CSIC), Cantoblanco, E-28049 Madrid, Spain*

E. E. Mendez

*Department of Physics and Astronomy, State University of New York at Stony Brook, Stony Brook, NY 11794-3800, USA*

N. Bojarczuk and S. Guha

*IBM Research Division, IBM Thomas J. Watson Research Center, P.O. Box 218, Yorktown Heights, NY 10598, USA*

(Received \* \* \*)

We have used Raman spectroscopy to study indium nitride thin films grown by molecular beam epitaxy on (111) silicon substrates at temperatures between 450° and 550°C. The Raman spectra show well defined peaks at 443, 475, 491, and 591 cm<sup>-1</sup>, which correspond to the  $A_1$ (TO),  $E_1$ (TO),  $E_2^{\text{high}}$ , and  $A_1$ (LO) phonons of the wurtzite structure, respectively. In backscattering normal to the surface the  $A_1$ (TO) and  $E_1$ (TO) peaks are very weak, indicating that the films grow along the hexagonal  $c$  axis. The dependence of the peak width on growth temperature reveals that the optimum temperature is 500°C, for which the fullwidth of the  $E_2^{\text{high}}$  peak has the minimum value of 7 cm<sup>-1</sup>. This small value, comparable to previous results for InN films grown on sapphire, is evidence of the good crystallinity of the films.

PACS numbers: 78.30.Fs, 78.66.Fd, 81.05.Ea, 81.15.Hi

The III-V direct-gap semiconductor InN has been largely ignored because its low dissociation temperature makes it very difficult to grow. However, in the last few years there has been an increasing interest on the material due, to large extent, to the successful application of nitride compounds in ultraviolet-blue light-emitting diodes and lasers. In particular, InN has promising transport and optical properties. Its large drift velocity at room temperature could render it better than GaAs and GaN for field effect transistors.<sup>1</sup> Carrier capture by InN quantum dots has been adduced for the efficient emission of blue-violet commercial InGaN diode lasers.<sup>2</sup> InN/Si tandem solar cells have been proposed for increased efficiency.<sup>3</sup> Finally, the important quaternary alloy AlGaInN covers most of the visible spectrum, reaching the orange-red end for InN.

Due to the lack of suitable lattice-matched substrates, InN thin films have been grown mostly on sapphire, which is widely available. Although silicon would be preferable for device applications and integration with microelectronic integrated circuits, films grown directly on Si substrates are poorly oriented.<sup>4</sup> The reason is that In adatoms have a long migration length that causes the formation of InN islands during the initial stages. The exposed Si surface reacts with the nitrogen beam to produce amorphous SiN, hindering the growth of high quality InN.<sup>4,5</sup> An AlN buffer layer has been shown to improve the quality of InN films grown on sapphire<sup>6</sup> and also of GaN films on Si.<sup>7</sup> Since Al has a short migration length, a thin, uniform AlN layer can be grown, avoiding

the reaction of the substrate with the nitrogen beam.

As other nitrides, InN can crystallize with the wurtzite hexagonal or the zincblende cubic structures. Raman spectroscopy has been extensively used to determine the structure and the crystallinity of GaN. For InN, previous work has been limited to wurtzite films grown on (0001) sapphire<sup>8-10</sup> and zincblende films grown on (001) GaAs.<sup>11</sup>

In this paper we report the growth and characterization by Raman scattering of oriented, crystalline InN films. InN thin films were grown by molecular beam epitaxy on (111) Si substrates using a RF plasma nitrogen source. Three different samples were grown at substrate temperatures  $T_g$  of 450°, 500° and 550°C, respectively. A 10-nm-thick AlN buffer layer was deposited between the substrate and the InN layer. Under the optical microscope the films presented a domain-like morphology. The domain size increased with growth temperature. The film grown at 550°C showed a poor adherence to the substrate.

Room temperature Raman spectra were taken with a Renishaw Ramascope spectrometer, equipped with an Ar<sup>+</sup> ion laser as a light source operating at a wavelength of 514.5 nm and focused on the sample through an optical microscope. The power density on the surface was of the order of 100 kw/cm<sup>2</sup>. Light scattered by the sample was collected with the same microscope and analyzed with a single-grating spectrograph and a CCD detector. Reflected and elastically scattered light was blocked with

\*Electronic mail: far@icmm.csic.es

two holographic filters, which also removed most of the Raman spectrum below  $100\text{ cm}^{-1}$ .

Figure 1 shows the Raman spectra for the InN films grown at different temperatures. All samples exhibit four peaks characteristic of bulk InN. In addition, the  $550^\circ\text{C}$  sample shows some peaks originating from the silicon substrate (labelled Si in the figure), due to its deficient coverage. The other samples show no signal from the substrate, and none of the three spectra reveal any band coming from the AlN buffer layer.<sup>12</sup>

The zincblende structure (spatial group  $T_d^2 - F\bar{4}3m$ ) has only two Raman-active phonons  $F_2(\text{TO})$  and  $F_2(\text{LO})$ . The wurtzite structure (spatial group  $C_{6v}^4 - P6_3mc$ ), which is the most stable, has six Raman-active phonons,  $A_1(\text{TO})$ ,  $A_1(\text{LO})$ ,  $E_1(\text{TO})$ ,  $E_1(\text{LO})$ , and  $2E_2$ . Therefore the number of peaks observed in the spectra indicates that the wurtzite phase must be present.

Table I lists the positions of the peaks and their symmetry assignment. The strongest peaks correspond to the  $E_2^{\text{high}}$  phonon at around  $491\text{ cm}^{-1}$  and to the  $A_1(\text{LO})$  phonon at around  $591\text{ cm}^{-1}$ . The frequency of the  $E_2^{\text{high}}$  phonon is very close to the value of  $488\text{ cm}^{-1}$  reported for InN on sapphire.<sup>10</sup>

The peaks at  $443$  and  $475\text{ cm}^{-1}$  have been identified as the  $A_1(\text{TO})$  and the  $E_1(\text{TO})$  phonons, respectively, of the hexagonal phase. This assignment has been done by comparison with the intensities of good quality GaN Raman spectra and by following the trend of phonon frequencies in AlN and GaN.<sup>12,13</sup> The frequency of the  $A_1(\text{TO})$  phonon agrees well with the value of  $450\text{ cm}^{-1}$  calculated by Kim *et al.*<sup>14</sup> but is much lower than the value reported by Inushima *et al.*<sup>10</sup> who assigned it to a shoulder in the Raman spectrum at  $480\text{ cm}^{-1}$ . On the other hand, the frequency of the  $E_1(\text{TO})$  phonon coincides with the value of Inushima *et al.*<sup>10</sup> but disagrees with the value of  $580\text{ cm}^{-1}$  estimated by Kim *et al.*<sup>14</sup> Both the  $E_1(\text{TO})$  and the  $A_1(\text{TO})$  are forbidden for backscattering along the hexagonal  $c$  axis. The fact that these peaks are very weak indicates that the films grow with a preferential orientation of this axis normal to the substrate plane.

The  $A_1(\text{LO})$  peak at  $591\text{ cm}^{-1}$  shows a low energy tail whose intensity depends on the sample and even on the measuring point. It could arise from the appearance of the forbidden mode  $E_1(\text{LO})$ , which has been reported<sup>10</sup> to be at  $570\text{ cm}^{-1}$ . Alternatively, the low-energy tail can be attributed to LO-phonon-plasmon coupling due to residual free carriers, whose concentration increases with increasing growth temperature. This interpretation would explain the observed increase of the continuous background with temperature, an effect that has been associated in GaN with an increasing dopant density.<sup>15</sup>

The full-width at half maximum (FWHM) of the  $E_2^{\text{high}}$  Raman peak, which varies from  $13$  to  $7\text{ cm}^{-1}$  (see Table I), depends on the crystallinity of the films. Usually, the peak is broadened by reduced phonon coherence caused by lattice disorder, the formation of nanocrystals or the presence of defects and impurities. The

observed linewidth indicates that the best crystallinity is obtained for a growth temperature of  $500^\circ\text{C}$ . The FWHM value of  $7\text{ cm}^{-1}$  at this temperature is comparable to the value of  $5\text{ cm}^{-1}$  observed for the best films grown on sapphire.<sup>9,16</sup> Although the latter has been preferred among the lattice-mismatched substrates, our results show that buffered silicon can also produce InN films with good crystallinity. This offers the advantage of a better compatibility with microelectronic integrated circuits and other silicon-based devices.

In summary, by depositing a thin AlN buffer layer we have been able to grow InN films with good crystallinity on Si substrates by molecular beam epitaxy. An analysis of their Raman spectra show that the films have a wurtzite structure with the hexagonal  $c$  axis perpendicular to the substrate plane. The best crystallinity of the samples is achieved for a growth temperature of (or close to)  $500^\circ\text{C}$ .

We acknowledge financial support from the Spanish CICYT (Projects MAT96-0395-CP and MAT97-0725) and the US Army Research Office. We thank C. Pecharomán for helpful discussions.

---

<sup>1</sup> S. K. O'Leary, B. E. Foutz, M. S. Shur, U. V. Bhapkar, and L. F. Eastman, *J. Appl. Phys.* **83**, 826 (1998).

<sup>2</sup> K. P. O'Donnell, R. W. Martin, and P. G. Middleton, *Phys. Rev. Lett.* **82**, 237 (1999).

<sup>3</sup> A. Yamamoto, M. Tsujino, M. Ohkubo, and A. Hashimoto, *Solar Energ. Mater. Solar Cells* **35**, 53 (1994).

<sup>4</sup> A. Yamamoto, M. Tsujino, M. Ohkubo, and A. Hashimoto, *J. Cryst. Growth* **137**, 415 (1994).

<sup>5</sup> I. Bello, W. M. Lau, R. P. W. Lawson, and K. K. Foo, *J. Vac. Sci. Technol.* **10**, 1642 (1992).

<sup>6</sup> T. J. Kistenmacher and W. A. Bryden, *Appl. Phys. Lett.* **59**, 1844 (1991).

<sup>7</sup> A. Watanabe, T. Takeuchi, K. Hirosawa, H. Amano, K. Hiramatsu, and I. Akasaki, *J. Cryst. Growth* **128**, 391 (1993).

<sup>8</sup> H.-J. Kwon, Y.-H. Lee, O. Miki, H. Yamano, and A. Yoshida, *Appl. Phys. Lett.* **69**, 937 (1996).

<sup>9</sup> M.-C. Lee, H.-C. Lin, Y.-C. Pan, C.-K. Shu, J. Ou, W.-H. Chen, and W.-K. Chen, *Appl. Phys. Lett.* **73**, 2606 (1998).

<sup>10</sup> T. Inushima, T. Shiraishi, and V. Y. Davydov, *Solid State Comm.* **110**, 491 (1999).

<sup>11</sup> A. Tabata, A. P. Lima, L. K. Teles, L. M. R. Scolfaro, J. R. Leite, V. Lemos, B. Schöttker, T. Frey, D. Schikora, and K. Lischka, *Appl. Phys. Lett.* **74**, 362 (1999).

<sup>12</sup> L. E. McNeil, M. Grimsditch, and R. H. French, *J. Am. Ceram. Soc.* **76**, 1132 (1993).

<sup>13</sup> F. A. Ponce, J. W. Steeds, C. D. Dyer, and G. D. Pitt, *Appl. Phys. Lett.* **69**, 2650 (1996).

<sup>14</sup> K. Kim, W. R. L. Lambrecht, and B. Segall, *Phys. Rev. B* **53**, 16310 (1996).

<sup>15</sup> H. Harima, T. Inoue, S. Nakashima, K. Furukawa, and M. Taneya, *Appl. Phys. Lett.* **73**, 2000 (1998).

<sup>16</sup> Y.-C. Pan, W.-H. Lee, C.-K. Shu, H.-C. Lin, C.-I. Chiang, H. Chang, D.-S. Lin, M.-C. Lee, and W.-K. Chen, Jpn. J. Appl. Phys. (Pt. 1) **38**, 645 (1999).

TABLE I. Summary of Raman phonon frequencies in  $\text{cm}^{-1}$  for the InN thin films grown on Si at different substrate temperatures  $T_g$ . The full widths of the peaks at half maximum are given in parenthesis in  $\text{cm}^{-1}$ . The symmetry species are for the wurtzite structure.

| $T_g$ ( $^{\circ}\text{C}$ ) | 450     | 500     | 550     |
|------------------------------|---------|---------|---------|
| $A_1(\text{TO})$             | 445(17) | 443(10) | 441(14) |
| $E_1(\text{TO})$             | 475(17) | 475(8)  | 471(14) |
| $E_2^{\text{high}}$          | 491(10) | 491(7)  | 489(13) |
| $A_1(\text{LO})$             | 590     | 591     | 588     |

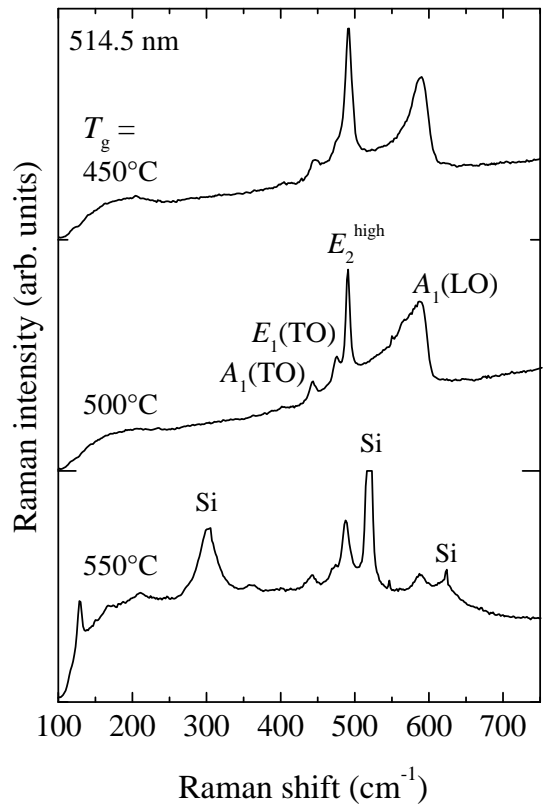


FIG. 1. Raman spectra for the InN thin films grown at three substrate temperatures  $T_g$ . The spectra have been shifted vertically for clarity. Ticks on the vertical axis mark the zero level for each case. Peaks originating in the substrate are labelled as Si.